Astroparticle Physics 84 (2016) 23–28

Contents lists available at ScienceDirect

Astroparticle Physics

journal homepage: www.elsevier.com/locate/astropartphys

Calibration of the Cherenkov telescope array using cosmic ray electrons

R.D. Parsons*, J.A. Hinton, H. Schoorlemmer

Max-Planck-Institut für Kernphysik, P.O. Box 103980, D 69029, Heidelberg, Germany

ARTICLE INFO

Article history:
Received 6 May 2016
Revised 1 July 2016
Accepted 2 August 2016
Available online 3 August 2016

Keywords:
Electron–positron spectrum
Imaging atmospheric Cherenkov telescopes
Calibration
CTA
Gamma rays

ABSTRACT

Cosmic ray electrons represent a background for gamma-ray observations with Cherenkov telescopes, initiating air-showers which are difficult to distinguish from photon-initiated showers. This similarity, however, and the presence of cosmic ray electrons in every field observed, makes them potentially very useful for calibration purposes. Here we study the precision with which the relative energy scale and collection area/efficiency for photons can be established using electrons for a major next generation instrument such as CTA. We find that variations in collection efficiency on hour timescales can be corrected to better than 1%. Furthermore, the break in the electron spectrum at $\sim$ 0.9 TeV can be used to calibrate the energy scale at the 3% level on the same timescale. For observations on the order of hours, statistical errors become negligible below a few TeV and allow for an energy scale cross-check with instruments such as CALET and AMS. Cosmic ray electrons therefore provide a powerful calibration tool, either as an alternative to intensive atmospheric monitoring and modelling efforts, or for independent verification of such procedures.

1. Introduction

Electrons (and positrons) represent $<$ 1% of the cosmic ray flux at 100 GeV energy. However, after the hadron-rejection cuts typically applied to date taken by Cherenkov telescope arrays, they represent a dominant background over a wide energy range, with improving hadron rejection compensating for the steeper electron spectrum ($\sim E^{-3}$ versus $\sim E^{-2.7}$) up to the break in the electron spectrum at 900 GeV [1]. The electron background is uniform on the sky at the $<$ 5% level below 100 GeV [2], while at higher energies the anisotropy is unknown (although anisotropy is expected to increase with energy). Electrons are therefore present in every field observed by Cherenkov telescope arrays, with close to isotropic flux, and separable from protons and nuclei using modern background-rejection methods [1,3–6]. Once the electron spectrum is known, the rate and spectrum measured in a given observation can be used to correct for atmospheric and instrumental deviations from the ideal case, or to check that atmospheric and instrumental corrections have been successfully applied. The advantages over cosmic ray protons and nuclei for this purpose (see for example [7]) are the close similarity of gamma and electron initiated air showers in terms of morphology and atmospheric depth at which the maximum number of particles is reached, albeit with a half radiation length shift, and the presence of a distinct feature in the CR electron spectrum: the 0.9 TeV break. This feature raises the prospect of independently establishing collection area and energy scale changes, something which is impossible using single power-law spectra. The spectral break position and level of high energy anisotropy in electrons will be established independently by future ground-based Cherenkov telescope arrays and by space-based instruments such as CALET [8] and perhaps AMS [9], providing a means for cross-calibration of the instrument based on a independent energy scale.

Measuring the cosmic ray electron spectrum with an array of Imaging Atmospheric Cherenkov Telescopes (IACTs) is, however, a significant challenge. The H.E.S.S. collaboration was the first to demonstrate that this is at all possible, by applying hard selection cuts (four telescope multiplicity and a random forest approach) [1]. Subsequently, these measurements were extended to lower energies for H.E.S.S. [10] and now confirmed by MAGIC [11] and VERITAS [12]. For current-generation instruments these measurements require long exposures: typically many hundreds of hours. Spectral measurements for gamma-ray sources make use of background estimates established using regions in the field of view thought to be empty of gamma-ray emission. This approach is clearly not possible for electrons, which are close to isotropic. Instead a model of the background in terms of some separation parameter (for example the output of a neural network classifier)

* Corresponding author.
E-mail address: daniel.parsons@mpi-hd.mpg.de (R.D. Parsons).

http://dx.doi.org/10.1016/j.astropartphys.2016.08.001
0927-6505/

must be established. This requires a detailed understanding of the development of hadronic cascades in the Earth's atmosphere. Significant differences exist (at the ∼ 10% level) between hadronic interaction models (or Monte–Carlo event/interaction generators) due to underlying physical uncertainties, particularly in the production of pions with a large forward momentum in the energy range of interest [13,14]. Dedicated instruments at the LHC, such as LHCf and TOTEM, as well as the general purpose ATLAS and CMS detectors, have now significantly reduced the uncertainties in this energy range and models such as EPOS LHC and QGSJETII are currently being refined to reflect these developments [15,16]. The systematic uncertainties on electron spectrum extraction will therefore be much smaller in the near future than those presented in the existing IACT publications.

The next generation facility CTA (the Cherenkov Telescope Array [17]) will employ over 100 telescopes at two sites (CTA-North and CTA-South), dramatically improving on the performance of current generation IACTs. The wider field of view of CTA telescopes (∼8° diameter), lower energy threshold (∼20 GeV), and very large collection area of the instrument (typically an order of magnitude larger than current instruments for gamma ray analyses, and even more for electron analyses due to the hard cuts often used, at all energies) [18] combine to produce an electron rate after quality selection cuts that is two or more orders of magnitude larger than that measured by current arrays [19] at ∼0.9 TeV. Furthermore, the background rejection power of CTA will be superior to that of current generation instruments, allowing the extraction of the cosmic ray electron spectrum over a wide energy range in a short time, with modest systematic uncertainties [19].

CTA will employ LIDAR-based atmospheric monitoring systems to measure variation in light propagation through the atmosphere ([20], and references therein). Whilst these measurements will be used to ensure realistic atmospheric treatment in the Monte Carlo simulation of the detector response, it is highly desirable to have a procedure for continuous confirmation that such measurement procedures have been successful, and as an independent means of deriving correction factors. In addition, instrumental effects may change the efficiency with which gamma-like showers trigger the array and pass selection cuts, and/or lead to systematic under or over estimation of photon energy. Again, CTA will make use of multiple methods to characterise such effects, but the approach of deriving the cosmic ray electron spectrum in a routine way for all observations without a significant diffuse gamma-ray component promises a convenient end-to-end method to establish correct performance or to derive correction factors. Due to the lack of bright diffuse gamma-ray emission in the relevant energy range and the small angular size of point-like sources compared to the instrument field-of-view, the electron spectrum can be extracted from almost all potential CTA extragalactic observations without the addition of an gamma-ray electron separation, simply by the removal of significant point sources from a given observation set (typically 1 source per field in the current generation of telescopes).

Here, we propose a method for a CTA electron spectrum measurement and assess the timescales on which the flux normalisation and break energy can be found. We go on to discuss the systematic uncertainties associated with this approach and its merits for the array-level calibration of CTA.

2. Approach

To test the feasibility of using the electron spectrum as a means of high level calibration, electron spectral measurements were simulated using the CTA-South "Production-2" Monte Carlo dataset [18]. Array layout "2Q" was used, which contains 4 large sized telescopes (23 m diameter), 24 medium sized telescopes (12 m) and 72 small sized telescopes (4 m). Direction and energy reconstruction were performed using the CTA baseline analysis,[1] under the assumption that the events are diffuse electrons. To ensure the quality of the images that are used in the reconstruction, we apply cuts on the number of pixels and number of photo-electrons (p.e.), these selection criteria were optimised for the nominal night-sky background rate (extrapolated from measurements at the H.E.S.S. site) and are summarised in Table 1 for each telescope type. To improve the quality of the reconstructed air shower parameters we require that the reconstructed shower direction lies within 4° of the telescope pointing direction and that a minimum of four telescopes participated in the reconstruction.

Table 1
Image cuts for the different type of telescopes.

Type	Amplitude (p.e.)	N_{pix}
Large (4)	>92.7	≥5
Medium (24)	>90.6	≥4
Small (72)	>29.5	≥4

An artificial neural network was created using the TMVA package [22] to perform classification of electrons from protons. The neural network was trained in five energy bins covering the full energy range of the CTA instrument (0.02–100 TeV), using the following discriminating variables:

- Mean scaled event width/length (see e.g. [23])
- Root mean square of scaled event width/length between telescopes
- Root mean square of event energy estimates between telescopes
- Reconstructed depth of shower maximum (X_{max})
- Spread of X_{max} estimates between telescopes
- Mean time gradient across an image [24]

Once trained, an independent sample of simulated data was passed through the network to produce the expected classifier (ζ) distributions of electrons and protons. Combining these distributions with the correct normalisations to provide the expected distribution of events when observing a gamma-ray free region of the sky requires assumptions on the spectra of protons and electrons, for which we adopt the following functional form for protons (based on data from [25]):

$$F_p = \phi_{0,\mathrm{p}}\left(\frac{E}{1\,\mathrm{TeV}}\right)^{\Gamma} \tag{1}$$

with $\phi_{0,\mathrm{p}} = 9.6\times10^{-2}\,\mathrm{m}^{-2}\mathrm{s}^{-1}\mathrm{TeV}^{-1}\mathrm{sr}^{-1}$ and $\Gamma = -2.7$. For electrons we have

$$F_e = \phi_{0.\mathrm{e}}\left(\frac{E}{1\,\mathrm{TeV}}\right)^{\Gamma_1}\left[1+\left(\frac{E}{E_b}\right)^{\frac{1}{\alpha}}\right]^{(\Gamma_2-\Gamma_1)\alpha} \tag{2}$$

with $\phi_{0,\mathrm{e}} = 1.5\times10^{-4}\,\mathrm{m}^{-2}\mathrm{s}^{-1}\mathrm{TeV}^{-1}\mathrm{sr}^{-1}$, $\Gamma_1 = -3.0$, $\Gamma_2 = -4.1$, $E_b = 0.9\,\mathrm{TeV}$, and $\alpha = 0.2$ (the H.E.S.S. measurement gives a limit of $\alpha < 0.3$), consistent with measurements using Fermi-LAT [2], AMS [9] and H.E.S.S. [10] respectively. The contribution of heavier cosmic-ray nuclei can be safely ignored, due to their lower expected fluxes and the extremely powerful background rejection for such events. This "data" distribution can then be scaled and Poisson fluctuations added to represent any length of observation time. Once this simulated observation expectation has been created, we use a component fitting technique similar to that used in [1], using the aforementioned particle classifier distributions to estimate

[1] Consisting of Hillas parameterisation of images and a weighted combination of the intersection of image axes for direction reconstruction, and energy estimation using look-up tables [21].

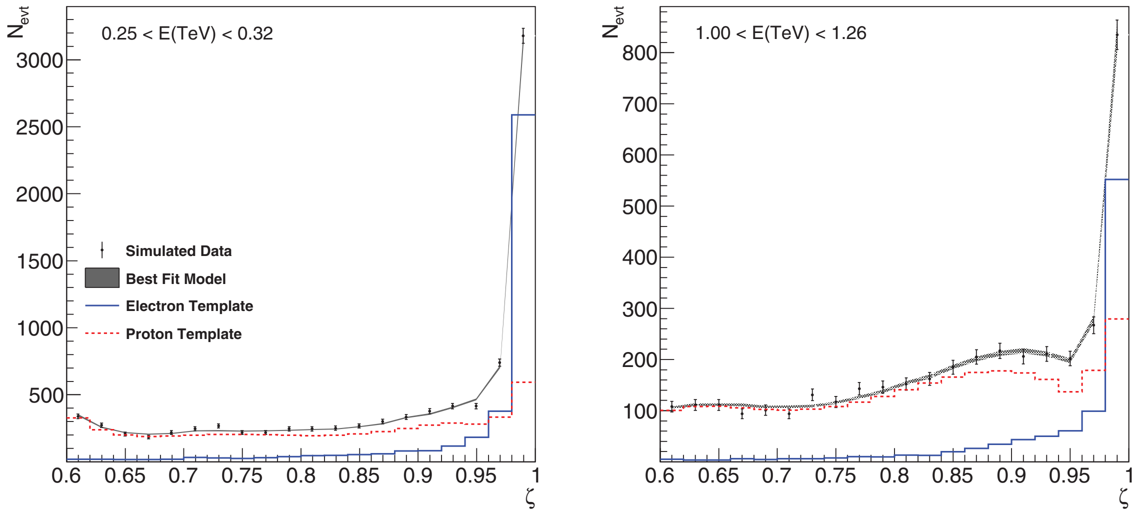

Fig. 1. Simulated distributions of the electron separation parameter ζ for an hour observation of a γ-ray source free region with CTA at an energy interval below (left) and above the (right) break E_b in the spectrum (proton distribution smoothed by polynomial fitting). The 1-σ error band of the best fitted model is also indicated.

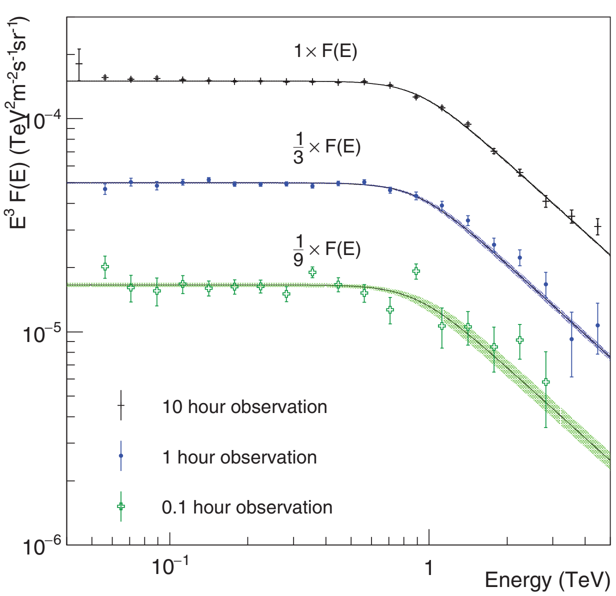

Fig. 2. Reconstructed electron spectra from simulations with CTA observations of different durations (scaled by different factors for readability). The markers illustrate the result from Monte Carlo simulation of a single observation run, while the lines and the shaded area indicate the average and the 68% confidence interval of the fitted spectrum from many Monte–Carlo realisations.

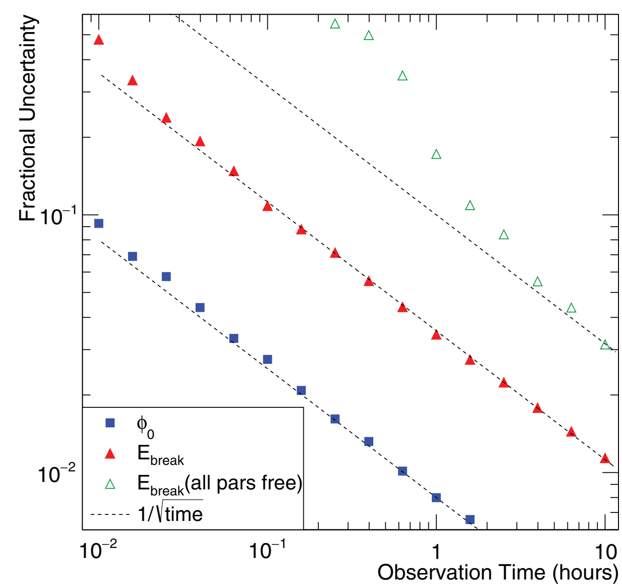

Fig. 3. Fractional statistical uncertainty on the reconstruction of spectral normalisation and energy break point as a function of observation time. For the break energy both the case of fixed spectral index before and after the break and the case with all parameters free are shown. In the background limited regime a $1/\sqrt{\text{time}}$ dependence is expected, illustrated by the dashed lines.

the contribution of each particle type to a given energy bin (see Fig. 1). The number of electrons in a given bin ($N_{\text{elec, i}}$) can then be estimated by integrating the fitted electron component. Fig. 1 gives examples of simulated and fitted ζ distributions, we selected one example below and one example above the energy at which the spectral break occurs.

Spectral fitting was performed using a forward folding technique [26], utilising the full energy migration matrix and effective area to produce the expected number of counts for a given spectrum. A minimisation was then performed using the MINUIT package[2] to find the values of the spectral constants where the expected distribution best matches $N_{\text{elec}}(E)$. Fig. 2 gives illustrative reconstructed electron spectra on different timescales.

[2] http://lcgapp.cern.ch/project/cls/work-packages/mathlibs/minuit/index.html.

3. Calibration accuracy

To test the accuracy of the spectral reconstruction 1000 realisations of the ζ distribution in each energy bin were created by adding random Poisson fluctuations to the expected event distributions. A spectral fit was then performed on each realisation, with the spectral index before and after the break fixed, but with break energy E_b and flux normalisation as free parameters. The standard deviation of the distribution of each parameter is taken as the uncertainty of that parameter for a given observation time.

Fig. 3 shows the evolution of the fractional uncertainty in both the normalisation and break point of the spectrum as a function of observation duration. One can see that the uncertainty on the normalisation drops rapidly with time, reaching the 10% level after only $\approx$ 1 min. This rapid improvement in accuracy is achievable as it is possible to calculate the normalisation from only the low energy data, allowing high statistics observations to be made in a relatively short time period.

The accuracy of the measurement of the break point improves more slowly, taking around 15 min to reach a 10% accuracy. This difference is due to the requirement of data points reconstructed above 0.9 TeV in order to resolve the break. Fig. 3 also shows the break point determination is all spectral parameters are left free (used for example for the measurement of the electron reference spectrum) the time taken to determine the cut-off to the 10% level is almost a factor of 10 larger, demonstrating the power of having a well known spectral shape. Further study of the accuracy when using only individual telescope subsystems, shows that the accuracy of this calibration in the most part derives from the MST subsystem, reaching 10% accuracy in almost the same time as the full system. This is most likely due to the large effective area in the region of the energy break of this subsystem. Whereas the LST subsystem with its much smaller effective area takes around five times longer. While the SST subsystem can take over ten times as long to calibrate to the 10% level, due to the threshold of this system being close to the energy break point.

It should be noted that the current measurement of the electron spectrum has relatively large systematic and statistical uncertainties at high energies, which leads to a fairly large uncertainties on the required timescales for determination of the break energy. For example, if the break energy is 20% higher than assumed here, the required observation time to reach a given accuracy would increase by a factor ~ 3.

4. Discussion

The results of Section 3 indicate that rapid electron spectral reconstruction should be possible with a next generation IACT array, such as the Southern and Northern CTA arrays. However, it is important to consider the impact of systematics on the electron spectral measurement and consequently the use of cosmic ray electrons for calibration purposes.

The model of calibration using this technique is first to construct a reference electron dataset based on the best atmospheric quality observations. This reference dataset can be used to generate a spectral model and if significant anisotropy exists in the reference set, or is established by CALET on this timescale, a directional model as well. The model can then be compared to the nightwise spectrum, after correction for atmospheric effects. This comparison provides an important check of the stability of the CTA spectral results over the lifetime of the array and under all atmospheric conditions.

The absolute reference spectrum is affected by several systematic effects, but in general the relative calibration factors determined by comparison to the reference are much less susceptible to systematics. The primary systematic uncertainties are expected to be:

- Uncertainties on the classifier distributions for proton showers, due to underlying uncertainties in **hadronic interactions**. Such uncertainties will be reduced over the coming decades with data from the LHC, but are unlikely to become negligible.
- **Atmospheric uncertainties** in a given data set are of course one of the main targets of the electron calibration, but uncertainties in the average atmospheric conditions during best possible observing conditions lead to systematics in the reference spectrum. CTA plans for a thorough characterisation of the atmosphere and hence such uncertainties should be greatly reduced with respect to current IACTs.
- **Detector model/simulation uncertainties** can be reduced over time with careful monitoring as planned for CTA, and an iterative approach with the many calibration tools available. Such uncertainties can also affect the behaviour of the background rejection classifier (for example in regions of high night sky background noise) and care must be taken to ensure the stability of such classifiers using Monte Carlo simulations under different potential observing conditions.
- Any significant cosmic-ray electron **anisotropy** will clearly lead initially to calibration uncertainties for individual pointings, but once established can be modelled and accounted for. The only problematic case is small scale anisotropy at a level of several percent, something which is not to our knowledge predicted by any model.

Many systematic checks are possible to help understand any deviations of measured spectra from the reference, or the reference spectrum from space-based measurements. The available data can for example be split into zenith and azimuth bands, into different telescope sub-systems (large, medium and small size telescopes) and different seasons, due to the very high statistics obtained overall.

The advantages of this approach over more traditional methods are the end-to-end nature of the calibration, sensitive to instrumental and atmospheric changes, the similarity of electrons to gamma rays and hence minimisation of systematics associated with extrapolation from the rather different hadronic showers, and the spectral feature, allowing collection area and energy-scale effects to be readily separated. Additionally, due to the very high cosmic ray electron statistics available from CTA it is possible to compare the electron spectrum reconstructed from arbitrary subsets of telescopes, allowing further systematic uncertainties to be probed (e.g. differing atmospheric absorption across the array footprint). Although not directly investigated here it should also be possible to perform such a calibration at the northern CTA site, due to the dominance in the calibration of the MSTs which CTA-North should have in similar numbers. The combination of data from ground-level muons with electrons is particularly powerful, with muons providing a means to calibrate individual telescopes [20,27], and electrons the system as a whole. Both muons and electrons will be collected during routine IACT observations and hence the downtime of the observatory due to special calibration runs is minimised.

5. Conclusions

Tests of electron spectral reconstruction demonstrate that a measurement of the relative normalisation and energy scaling factor of the cosmic-ray electron spectrum is possible at the 3% level with under one hour of CTA observations. Such short timescale measurements make it possible to use the electron background seen in all observation runs as a “standard candle”, allowing the systematics of the gamma-ray spectral reconstruction of CTA to be assessed over the lifetime of the instrument. This technique can be used in concert with the several absolute calibration techniques for the atmosphere, individual telescopes, and for the full array, that have been proposed for CTA [20]. Together with point spread function verification using point-like gamma-ray sources (for example blazar flares), this procedure can be used as a high level check of the “health” of the instrument over its expected 30 year operational lifetime, ensuring absolute data corrections remain consistent and spectral results are stable. This conclusion can of course be extended from CTA to any instrument with substantially improved sensitivity and field of view with respect to current IACTs.

Acknowledgements

This work was done as part of a major simulations and calibration effort for CTA, and hence draws on the work and expertise

of many members of the CTA consortium. This paper has gone through internal review by the CTA Consortium.

References

[1] F. Aharonian, A.G. Akhperjanian, U. Barres de Almeida, A.R. Bazer-Bachi, Y. Becherini, B. Behera, W. Benbow, K. Bernlöhr, C. Boisson, A. Bochow, V. Borrel, I. Braun, E. Brion, J. Brucker, P. Brun, R. Bühler, T. Bulik, I. Büsching, T. Boutelier, S. Carrigan, P.M. Chadwick, A. Charbonnier, R.C.G. Chaves, A. Cheesebrough, L.-M. Chounet, A.C. Clapson, G. Coignet, L. Costamante, M. Dalton, B. Degrange, C. Deil, H.J. Dickinson, A. Djannati-Ataï, W. Domainko, L.O.. Drury, F. Dubois, G. Dubus, J. Dyks, M. Dyrda, K. Egberts, D. Emmanoulopoulos, P. Espigat, C. Farnier, F. Feinstein, A. Fiasson, A. Förster, G. Fontaine, M. Füßling, S. Gabici, Y.A. Gallant, L. Gérard, B. Giebels, J.F. Glicenstein, B. Glück, P. Goret, C. Hadjichristidis, D. Hauser, M. Hauser, S. Heinz, G. Heinzelmann, G. Henri, G. Hermann, J.A. Hinton, A. Hoffmann, W. Hofmann, M. Holleran, S. Hoppe, D. Horns, A. Jacholkowska, O.C. de Jager, I. Jung, K. Katarzyński, S. Kaufmann, E. Kendziorra, M. Kerschhaggl, D. Khangulyan, B. Khélifi, D. Keogh, N. Komin, K. Kosack, G. Lamanna, J.-P. Lenain, T. Lohse, V. Marandon, J.M. Martin, O. Martineau-Huynh, A. Marcowith, D. Maurin, T.J.L. McComb, C. Medina, R. Moderski, E. Moulin, M. Naumann-Godo, M. de Naurois, D. Nedbal, D. Nekrassov, J. Niemiec, S.J. Nolan, S. Ohm, J.-F. Olive, E. de Oña Wilhelmi, K.J. Orford, J.L. Osborne, M. Ostrowski, M. Panter, G. Pedaletti, G. Pelletier, P.-O. Petrucci, S. Pita, G. Pühlhofer, M. Punch, A. Quirrenbach, B.C. Raubenheimer, M. Raue, S.M. Rayner, M. Renaud, F. Rieger, J. Ripken, L. Rob, S. Rosier-Lees, G. Rowell, B. Rudak, C.B. Rulten, J. Ruppel, V. Sahakian, A. Santangelo, R. Schlickeiser, F.M. Schöck, R. Schröder, U. Schwanke, S. Schwarzburg, S. Schwemmer, A. Shalchi, J.L. Skilton, H. Sol, D. Spangler, Ł. Stawarz, R. Steenkamp, C. Stegmann, G. Superina, P.H. Tam, J.-P. Tavernet, R. Terrier, O. Tibolla, C. van Eldik, G. Vasileiadis, C. Venter, J.P. Vialle, P. Vincent, M. Vivier, H.J. Völk, F. Volpe, S.J. Wagner, M. Ward, A.A. Zdziarski, A. Zech, Energy spectrum of cosmic-ray electrons at TeV energies, Phys. Rev. Lett. 101 (26) (2008) 261104, doi:10.1103/PhysRevLett.101.261104.

[2] M. Ackermann, M. Ajello, W.B. Atwood, L. Baldini, J. Ballet, G. Barbiellini, D. Bastieri, K. Bechtol, R. Bellazzini, B. Berenji, E.D. Bloom, E. Bonamente, A.W. Borgland, A. Bouvier, J. Bregeon, A. Brez, M. Brigida, P. Bruel, R. Buehler, T.H. Burnett, S. Buson, G.A. Caliandro, R.A. Cameron, P.A. Caraveo, S. Carrigan, J.M. Casandjian, C. Cecchi, Ö. Çelik, E. Charles, A. Chekhtman, C.C. Cheung, J. Chiang, S. Ciprini, R. Claus, J. Cohen-Tanugi, J. Conrad, A. Cuoco, C.D. Dermer, A. de Angelis, F. de Palma, S.W. Digel, G. di Bernardo, E. Do Couto E Silva, P.S. Drell, R. Dubois, C. Favuzzi, S.J. Fegan, W.B. Focke, M. Frailis, Y. Fukazawa, S. Funk, P. Fusco, D. Gaggero, F. Gargano, S. Germani, N. Giglietto, P. Giommi, F. Giordano, M. Giroletti, T. Glanzman, G. Godfrey, D. Grasso, I.A. Grenier, J.E. Grove, S. Guiriec, M. Gustafsson, D. Hadasch, A.K. Harding, K. Hayashi, E. Hays, R.E. Hughes, G. Jóhannesson, A.S. Johnson, W.N. Johnson, T. Kamae, H. Katagiri, J. Kataoka, M. Kerr, J. Knödlseder, M. Kuss, J. Lande, L. Latronico, S.-H. Lee, M. Lemoine-Goumard, M. Llena Garde, F. Longo, F. Loparco, M.N. Lovellette, P. Lubrano, A. Makeev, M.N. Mazziotta, J.E. McEnery, J. Mehault, P.F. Michelson, T. Mizuno, A.A. Moiseev, C. Monte, M.E. Monzani, E. Moretti, A. Morselli, I.V. Moskalenko, S. Murgia, T. Nakamori, M. Naumann-Godo, P.L. Nolan, E. Nuss, T. Ohsugi, A. Okumura, N. Omodei, E. Orlando, J.F. Ormes, D. Paneque, J.H. Panetta, D. Parent, V. Pelassa, M. Pepe, M. Pesce-Rollins, F. Piron, T.A. Porter, S. Profumo, S. Rainò, R. Rando, M. Razzano, A. Reimer, O. Reimer, T. Reposeur, J. Ripken, S. Ritz, M. Roth, H.F.-W. Sadrozinski, A. Sander, T.L. Schalk, C. Sgrò, J. Siegal-Gaskins, E.J. Siskind, D.A. Smith, P.D. Smith, G. Spandre, P. Spinelli, M.S. Strickman, A.W. Strong, D.J. Suson, H. Takahashi, T. Takahashi, T. Tanaka, J.B. Thayer, J.G. Thayer, D.J. Thompson, L. Tibaldo, D.F. Torres, G. Tosti, A. Tramacere, Y. Uchiyama, T.L. Usher, J. Vandenbroucke, V. Vasileiou, N. Vilchez, V. Vitale, A.P. Waite, P. Wang, B.L. Winer, K.S. Wood, Z. Yang, T. Ylinen, G. Zaharijas, M. Ziegler, Searches for cosmic-ray electron anisotropies with the fermi large area telescope, Phys. Rev. D 82 (9) (2010) 092003, doi:10.1103/PhysRevD.82.092003.

[3] J. Albert, E. Aliu, H. Anderhub, P. Antoranz, A. Armada, M. Asensio, C. Baixeras, J.A. Barrio, H. Bartko, D. Bastieri, J. Becker, W. Bednarek, K. Berger, C. Bigongiari, A. Biland, R.K. Bock, P. Bordas, V. Bosch-Ramon, T. Bretz, I. Britvitch, M. Camara, E. Carmona, A. Chilingarian, S. Ciprini, J.A. Coarasa, S. Commichau, J.L. Contreras, J. Cortina, M.T. Costado, V. Curtef, V. Danielyan, F. Dazzi, A. de Angelis, C. Delgado, R. de Los Reyes, B. de Lotto, E. Domingo-Santamaría, D. Dorner, M. Doro, M. Errando, M. Fagiolini, D. Ferenc, E. Fernández, R. Firpo, J. Flix, M.V. Fonseca, L. Font, M. Fuchs, N. Galante, R.J. García-López, M. Garczarczyk, M. Gaug, M. Giller, F. Goebel, D. Hakobyan, M. Hayashida, T. Hengstebeck, A. Herrero, D. Höhne, J. Hose, S. Huber, C.C. Hsu, P. Jacon, T. Jogler, R. Kosyra, D. Kranich, R. Kritzer, A. Laille, E. Lindfors, S. Lombardi, F. Longo, J. López, M. López, E. Lorenz, P. Majumdar, G. Maneva, K. Mannheim, M. Mariotti, M. Martínez, D. Mazin, C. Merck, M. Meucci, M. Meyer, J.M. Miranda, R. Mirzoyan, S. Mizobuchi, A. Moralejo, D. Nieto, K. Nilsson, J. Ninkovic, E. Oña-Wilhelmi, N. Otte, I. Oya, M. Panniello, R. Paoletti, J.M. Paredes, M. Pasanen, D. Pascoli, F. Pauss, R. Pegna, M. Persic, L. Peruzzo, A. Piccioli, N. Puchades, E. Prandini, A. Raymers, W. Rhode, M. Ribó, J. Rico, M. Rissi, A. Robert, S. Rügamer, A. Saggion, T.Y. Saito, A. Sánchez, P. Sartori, V. Scalzotto, V. Scapin, R. Schmitt, T. Schweizer, M. Shayduk, K. Shinozaki, S.N. Shore, N. Sidro, A. Sillanpää, D. Sobczynska, F. Spanier, A. Stamerra, L.S. Stark, L. Takalo, P. Temnikov, D. Tescaro, M. Teshima, D.F. Torres, N. Turini, H. Vankov, A. Venturini, V. Vitale, R.M. Wagner, T. Wibig, W. Wittek, F. Zandanel, R. Zanin, J. Zapatero, Implementation of the random forest method for the imaging atmospheric Cherenkov telescope MAGIC, Nucl. Instrum. Methods Phys. Res. A 588 (2008) 424–432, doi:10.1016/j.nima.2007.11.068.

[4] S. Ohm, C. van Eldik, K. Egberts, γ/hadron separation in very-high-energy γ-ray astronomy using a multivariate analysis method, Astropart. Phys. 31 (2009) 383–391, doi:10.1016/j.astropartphys.2009.04.001.

[5] M. de Naurois, L. Rolland, A high performance likelihood reconstruction of γ-rays for imaging atmospheric Cherenkov telescopes, Astropart. Phys. 32 (2009) 231–252, doi:10.1016/j.astropartphys.2009.09.001.

[6] Y. Becherini, A. Djannati-Ataï, V. Marandon, M. Punch, S. Pita, A new analysis strategy for detection of faint γ-ray sources with imaging atmospheric Cherenkov telescopes, Astropart. Phys. 34 (2011) 858–870, doi:10.1016/j.astropartphys.2011.03.005.

[7] S. Lebohec, J. Holder, The cosmic ray background as a tool for relative calibration of atmospheric Cherenkov telescopes, Astropart. Phys. 19 (2003) 221–233, doi:10.1016/S0927-6505(02)00201-3.

[8] P.S. Marrocchesi, Calet Collaboration, CALET: a calorimeter-based orbital observatory for high energy astroparticle physics, Nucl. Instrum. Methods Phys. Res. A 692 (2012) 240–245, doi:10.1016/j.nima.2011.12.108.

[9] M. Aguilar, et al., Electron and positron fluxes in primary cosmic rays measured with the alpha magnetic spectrometer on the international space station, Phys. Rev. Lett. 113 (2014) 121102, doi:10.1103/PhysRevLett.113.121102.

[10] F. Aharonian, A.G. Akhperjanian, G. Anton, U. Barres de Almeida, A.R. Bazer-Bachi, Y. Becherini, B. Behera, K. Bernlöhr, A. Bochow, C. Boisson, J. Bolmont, V. Borrel, J. Brucker, F. Brun, P. Brun, R. Bühler, T. Bulik, I. Büsching, T. Boutelier, P.M. Chadwick, A. Charbonnier, R.C.G. Chaves, A. Cheesebrough, L.-M. Chounet, A.C. Clapson, G. Coignet, M. Dalton, M.K. Daniel, I.D. Davids, B. Degrange, C. Deil, H.J. Dickinson, A. Djannati-Ataï, W. Domainko, L. O'C.Drury, F. Dubois, G. Dubus, J. Dyks, M. Dyrda, K. Egberts, D. Emmanoulopoulos, P. Espigat, C. Farnier, F. Feinstein, A. Fiasson, A. Förster, G. Fontaine, M. Füßling, S. Gabici, Y.A. Gallant, L. Gérard, D. Gerbig, B. Giebels, J.F. Glicenstein, B. Glück, P. Goret, D. Göring, D. Hauser, M. Hauser, S. Heinz, G. Heinzelmann, G. Henri, G. Hermann, J.A. Hinton, A. Hoffmann, W. Hofmann, M. Holleran, S. Hoppe, D. Horns, A. Jacholkowska, O.C. de Jager, C. Jahn, I. Jung, K. Katarzyński, U. Katz, S. Kaufmann, E. Kendziorra, M. Kerschhaggl, D. Khangulyan, B. Khélifi, D. Keogh, W. Kluźniak, T. Kneiske, N. Komin, K. Kosack, R. Kossakowski, G. Lamanna, J.-P. Lenain, T. Lohse, V. Marandon, J.M. Martin, O. Martineau-Huynh, A. Marcowith, J. Masbou, D. Maurin, T.J.L. McComb, M.C. Medina, R. Moderski, E. Moulin, M. Naumann-Godo, M. de Naurois, D. Nedbal, D. Nekrassov, B. Nicholas, J. Niemiec, S.J. Nolan, S. Ohm, J.-F. Olive, E. de Oña Wilhelmi, K.J. Orford, M. Ostrowski, M. Panter, M. Paz Arribas, G. Pedaletti, G. Pelletier, P.-O. Petrucci, S. Pita, G. Pühlhofer, M. Punch, A. Quirrenbach, B.C. Raubenheimer, M. Raue, S.M. Rayner, O. Reimer, M. Renaud, F. Rieger, J. Ripken, L. Rob, S. Rosier-Lees, G. Rowell, B. Rudak, C.B. Rulten, J. Ruppel, V. Sahakian, A. Santangelo, R. Schlickeiser, F.M. Schöck, R. Schröder, U. Schwanke, S. Schwarzburg, S. Schwemmer, A. Shalchi, M. Sikora, J.L. Skilton, H. Sol, D. Spangler, Ł. Stawarz, R. Steenkamp, C. Stegmann, F. Stinzing, G. Superina, A. Szostek, P.H. Tam, J.-P. Tavernet, R. Terrier, O. Tibolla, M. Tluczykont, C. van Eldik, G. Vasileiadis, C. Venter, L. Venter, J.P. Vialle, P. Vincent, M. Vivier, H.J. Völk, F. Volpe, S.J. Wagner, M. Ward, A.A. Zdziarski, A. Zech, Probing the ATIC peak in the cosmic-ray electron spectrum with H.E.S.S., Astron. Astrophys. 508 (2009) 561–564, doi:10.1051/0004-6361/200913323.

[11] D. Borla Tridon, Measurement of the cosmic electron spectrum with the MAGIC telescopes, Int. Cosmic Ray Conf. 6 (2011) 47, doi:10.7529/ICRC2011/V06/0680.

[12] D. Staszak, for the VERITAS Collaboration, A Cosmic-ray Electron Spectrum with VERITAS, ArXiv e-prints (2015).

[13] D. d'Enterria, R. Engel, T. Pierog, S. Ostapchenko, K. Werner, Constraints from the first LHC data on hadronic event generators for ultra-high energy cosmic-ray physics, Astropart. Phys. 35 (2011) 98–113, doi:10.1016/j.astropartphys.2011.05.002.

[14] R.D. Parsons, C. Bleve, S.S. Ostapchenko, J. Knapp, Systematic uncertainties in air shower measurements from high-energy hadronic interaction models, Astropart. Phys. 34 (2011) 832–839, doi:10.1016/j.astropartphys.2011.02.007.

[15] S. Ostapchenko, Monte Carlo treatment of hadronic interactions in enhanced Pomeron scheme: QGSJET-II model, Phys. Rev. D 83 (1) (2011) 014018, doi:10.1103/PhysRevD.83.014018.

[16] T. Pierog, I. Karpenko, J.M. Katzy, E. Yatsenko, K. Werner, EPOS LHC: test of collective hadronization with data measured at the CERN large hadron collider, Phys. Rev. C92 (3) (2015) 034906, doi:10.1103/PhysRevC.92.034906.

[17] B.S. Acharya, M. Actis, T. Aghajani, G. Agnetta, J. Aguilar, F. Aharonian, M. Ajello, A. Akhperjanian, M. Alcubierre, J. Aleksić, et al., Introducing the CTA concept, Astropart. Phys. 43 (2013) 3–18, doi:10.1016/j.astropartphys.2013.01.007.

[18] T. Hassan, L. Arrabito, K. Bernlör, J. Bregeon, J. Hinton, T. Jogler, G. Maier, A. Moralejo, F. Di Pierro, M. Wood, f.t. CTA Consortium, Second large-scale Monte Carlo study for the Cherenkov telescope array, ArXiv e-prints (2015).

[19] R.D. Parsons, Towards a measurement of the cosmic ray electron spectrum at the highest energies (Ph.D. thesis), University of Leeds, 2011.

[20] M. Gaug, D. Berge, M. Daniel, M. Doro, A. FÃ¶rster, W. Hofmann, M.C. Maccarone, D. Parsons, R. de los Reyes Lopez, C. van Eldik, Calibration strategies for the Cherenkov telescope array, Proc. SPIE Int. Soc. Opt. Eng. 9149 (2014) 914919, doi:10.1117/12.2054536.

[21] K. Bernlöhr, A. Barnacka, Y. Becherini, O. Blanch Bigas, E. Carmona, P. Colin, G. Decerprit, F. Di Pierro, F. Dubois, C. Farnier, S. Funk, G. Hermann, J.A. Hinton, T.B. Humensky, B. Khélifi, T. Kihm, N. Komin, J.-P. Lenain, G. Maier, D. Mazin, M.C. Medina, A. Moralejo, S.J. Nolan, S. Ohm, E. de Oña Wilhelmi, R.D. Parsons, M. Paz Arribas, G. Pedaletti, S. Pita, H. Prokoph, C.B. Rulten,

U. Schwanke, M. Shayduk, V. Stamatescu, P. Vallania, S. Vorobiov, R. Wischnewski, T. Yoshikoshi, A. Zech, CTA Consortium, Monte Carlo design studies for the Cherenkov telescope array, Astropart. Phys. 43 (2013) 171–188, doi:10.1016/j.astropartphys.2012.10.002.

[22] A. Hoecker, P. Speckmayer, J. Stelzer, J. Therhaag, E. von Toerne, H. Voss, M. Backes, T. Carli, O. Cohen, A. Christov, D. Dannheim, K. Danielowski, S. Henrot-Versille, M. Jachowski, K. Kraszewski, A. Krasznahorkay, Jr., M. Kruk, Y. Mahalalel, R. Ospanov, X. Prudent, A. Robert, D. Schouten, F. Tegenfeldt, A. Voigt, K. Voss, M. Wolter, A. Zemla, TMVA - Toolkit for Multivariate Data Analysis, ArXiv Physics e-prints (2007).

[23] F. Aharonian, A.G. Akhperjanian, A.R. Bazer-Bachi, M. Beilicke, W. Benbow, D. Berge, K. Bernlöhr, C. Boisson, O. Bolz, V. Borrel, I. Braun, F. Breitling, A.M. Brown, R. Bühler, I. Büsching, S. Carrigan, P.M. Chadwick, L.-M. Chounet, R. Cornils, L. Costamante, B. Degrange, H.J. Dickinson, A. Djannati-Ataï, L. O'C.Drury, G. Dubus, K. Egberts, D. Emmanoulopoulos, P. Espigat, F. Feinstein, E. Ferrero, A. Fiasson, G. Fontaine, S. Funk, S. Funk, Y.A. Gallant, B. Giebels, J.F. Glicenstein, P. Goret, C. Hadjichristidis, D. Hauser, M. Hauser, G. Heinzelmann, G. Henri, G. Hermann, J.A. Hinton, W. Hofmann, M. Holleran, D. Horns, A. Jacholkowska, O.C. de Jager, B. Khélifi, N. Komin, A. Konopelko, K. Kosack, I.J. Latham, R. Le Gallou, A. Lemière, M. Lemoine-Goumard, T. Lohse, J.M. Martin, O. Martineau-Huynh, A. Marcowith, C. Masterson, T.J.L. McComb, M. de Naurois, D. Nedbal, S.J. Nolan, A. Noutsos, K.J. Orford, J.L. Osborne, M. Ouchrif, M. Panter, G. Pelletier, S. Pita, G. Pühlhofer, M. Punch, B.C. Raubenheimer, M. Raue, S.M. Rayner, A. Reimer, O. Reimer, J. Ripken, L. Rob, L. Rolland, G. Rowell, V. Sahakian, L. Saugé, S. Schlenker, R. Schlickeiser, U. Schwanke, H. Sol, D. Spangler, F. Spanier, R. Steenkamp, C. Stegmann, G. Superina, J.-P. Tavernet, R. Terrier, C.G. Théoret, M. Tluczykont, C. van Eldik, G. Vasileiadis, C. Venter, P. Vincent, H.J. Völk, S.J. Wagner, M. Ward, Observations of the crab nebula with HESS, Astron. Astrophys. 457 (2006) 899–915, doi:10.1051/0004-6361:20065351.

[24] E. Aliu, H. Anderhub, L.A. Antonelli, P. Antoranz, M. Backes, C. Baixeras, J.A. Barrio, H. Bartko, D. Bastieri, J.K. Becker, W. Bednarek, K. Berger, E. Bernardini, A. Biland, R.K. Bock, G. Bonnoli, P. Bordas, D. Borla Tridon, V. Bosch-Ramon, T. Bretz, I. Britvitch, M. Camara, E. Carmona, A. Chilingarian, S. Commichau, J.L. Contreras, J. Cortina, M.T. Costado, S. Covino, V. Curtef, F. Dazzi, A. de Angelis, E. de Cea Del Pozo, R. de Los Reyes, B. de Lotto, M. de Maria, F. de Sabata, C. Delgado Mendez, A. Dominguez, D. Dorner, M. Doro, D. Elsässer, M. Errando, M. Fagiolini, D. Ferenc, E. Fernández, R. Firpo, M.V. Fonseca, L. Font, N. Galante, R.J. García López, M. Garczarczyk, M. Gaug, F. Goebel, D. Hadasch, M. Hayashida, A. Herrero, D. Höhne, J. Hose, C.C. Hsu, S. Huber, T. Jogler, D. Kranich, A. La Barbera, A. Laille, E. Leonardo, E. Lindfors, S. Lombardi, F. Longo, M. López, E. Lorenz, P. Majumdar, G. Maneva, N. Mankuzhiyil, K. Mannheim, L. Maraschi, M. Mariotti, M. Martínez, D. Mazin, M. Meucci, M. Meyer, J.M. Miranda, R. Mirzoyan, M. Moles, A. Moralejo, D. Nieto, K. Nilsson, J. Ninkovic, N. Otte, I. Oya, R. Paoletti, J.M. Paredes, M. Pasanen, D. Pascoli, F. Pauss, R.G. Pegna, M.A. Perez-Torres, M. Persic, L. Peruzzo, A. Piccioli, F. Prada, E. Prandini, N. Puchades, A. Raymers, W. Rhode, M. Ribó, J. Rico, M. Rissi, A. Robert, S. Rügamer, A. Saggion, T.Y. Saito, M. Salvati, M. Sanchez-Conde, P. Sartori, K. Satalecka, V. Scalzotto, V. Scapin, T. Schweizer, M. Shayduk, K. Shinozaki, S.N. Shore, N. Sidro, A. Sierpowska-Bartosik, A. Sillanpää, J. Sitarek, D. Sobczynska, F. Spanier, A. Stamerra, L.S. Stark, L. Takalo, F. Tavecchio, P. Temnikov, D. Tescaro, M. Teshima, M. Tluczykont, D.F. Torres, N. Turini, H. Vankov, A. Venturini, V. Vitale, R.M. Wagner, W. Wittek, V. Zabalza, F. Zandanel, R. Zanin, J. Zapatero, Improving the performance of the single-dish Cherenkov telescope MAGIC through the use of signal timing, Astropart. Phys. 30 (2009) 293–305, doi:10.1016/j.astropartphys.2008.10.003.

[25] Y. Shikaze, S. Haino, K. Abe, H. Fuke, T. Hams, K.C. Kim, Y. Makida, S. Matsuda, J.W. Mitchell, A.A. Moiseev, J. Nishimura, M. Nozaki, S. Orito, J.F. Ormes, T. Sanuki, M. Sasaki, E.S. Seo, R.E. Streitmatter, J. Suzuki, K. Tanaka, T. Yamagami, A. Yamamoto, T. Yoshida, K. Yoshimura, Measurements of 0.2 20 GeV/n cosmic-ray proton and helium spectra from 1997 through 2002 with the BESS spectrometer, Astropart. Phys. 28 (2007) 154–167, doi:10.1016/j.astropartphys.2007.05.001.

[26] F. Piron, A. Djannati-Atai, M. Punch, J.-P. Tavernet, A. Barrau, R. Bazer-Bachi, L.-M. Chounet, G. Debiais, B. Degrange, J.-P. Dezalay, P. Espigat, B. Fabre, P. Fleury, G. Fontaine, P. Goret, C. Gouiffes, B. Khelifi, I. Malet, C. Masterson, G. Mohanty, E. Nuss, C. Renault, M. Rivoal, L. Rob, S. Vorobiov, Temporal and spectral gamma-ray properties of Mkn 421 above 250 GeV from CAT observations between 1996 and 2000, Astron. Astrophys. 374 (2001) 895–906, doi:10.1051/0004-6361:20010798.

[27] G. Vacanti, P. Fleury, Y. Jiang, E. Paré, A.C. Rovero, X. Sarazin, M. Urban, T.C. Weekes, Muon ring images with an atmospheric Čerenkov telescope, Astropart. Phys. 2 (1994) 1–11, doi:10.1016/0927-6505(94)90012-4.